Exploration of Myocardial Fiber Array Using Diffusion MR Tractography in Small Animal Heart Failure Model: Comparison with 3D Pathology Using Tissue-Clearing Technique

Sang-Eun Lee

Department of Medicine
The Graduate School, Yonsei University

Exploration of Myocardial Fiber Array Using Diffusion MR Tractography in Small Animal Heart Failure Model: Comparison with 3D Pathology Using Tissue-Clearing Technique

Directed by Professor Hyuk-Jae Chang

The Doctoral Dissertation
submitted to the Department of Medicine,
the Graduate School of Yonsei University
in partial fulfillment of the requirements for the degree
of Doctor of Philosophy

Sang-Eun Lee

December 2016

This certifies that the Doctoral Dissertation of Sang-Eun Lee is approved.

_____

Thesis Supervisor : Hyuk-Jae Chang

_____

Thesis Committee Member#1 : Chul Hoon Kim

_____

Thesis Committee Member#2 : Jin Hur

_____

Thesis Committee Member#3 : Eun Ju Chun

_____

Thesis Committee Member#4 : Eo-Jin Kim

The Graduate School
Yonsei University

December 2016

ACKNOWLEDGEMENTS

First and foremost, I would like to express my sincerest gratitude to my supervisor and mentor, Prof. Hyuk-Jae Chang, who has given me the opportunity to work with him and has made conducting this research possible, for his continuous guidance, patience, and motivation. I have furthermore to thank Prof. Chul Hoon Kim, Prof. Jin Hur, Prof. Eun Ju Chun, and Prof. Eo-Jin Kim, for their insightful comments and encouragement. My sincere thanks also go to Prof. Namsik Chung, Prof. Donghoon Choi, Prof. Seok-Min Kang, Prof. Debiao Li, Dr. Jong Jin Yoon, and Dr. Christopher Nguyen for all their help and support during the process. Last but not least, I would also like to thank my family for the support they provided me through my entire life.

<TABLE OF CONTENTS>

LIST OF FIGURES

ABSTRACT

Exploration of Myocardial Fiber Array Using Diffusion MR Tractography in Small Animal Heart Failure Model: Comparison with 3D Pathology Using Tissue-Clearing Technique

Sang-Eun Lee

Department of Medicine
The Graduate School, Yonsei University

(Directed by Professor Hyuk-Jae Chang)

Verifying the microarchitecture of the heart can improve understanding of the fundamental heart structure-function relationships both in normal development and cardiovascular disease progression. The current study demonstrate a novel approach to characterize the microstructural response of the myocardium to cardiovascular disease by interrogating intact, un-sectioned myocardium with 3-dimensional (3D) histological imaging using a tissue-clearing technique and quantifying myocardial fiber orientation. In the same samples, diffusion magnetic resonance imaging, a clinically translatable non-invasive imaging technique, was also applied to demonstrate its potential in yielding a surrogate marker for myocardial fiber orientation. Both 3D histological imaging and diffusion magnetic resonance imaging were significantly correlated in verifying the helical architecture of the normal myocardium and that this normal helical structure is perturbed in both ischemic and non-ischemic heart failure model.

Key words: myocardial fiber orientation, magnetic resonance imaging

Exploration of Myocardial Fiber Array Using Diffusion MR Tractography in Small Animal Heart Failure Model: Comparison with 3D Pathology Using Tissue-Clearing Technique

Sang-Eun Lee

Department of Medicine
The Graduate School, Yonsei University

(Directed by Professor Hyuk-Jae Chang)

I. INTRODUCTION

Myocardial structure is composed of muscle fibers organized in a twisting helix structure that can yield efficient pumping. The mammalian heart's largest chamber, left ventricle, was further revealed to contain laminar helical structures that continuously span from left-handed (epicardium) to right-handed (endocardium) orientation (**figure 1**).[1,2]

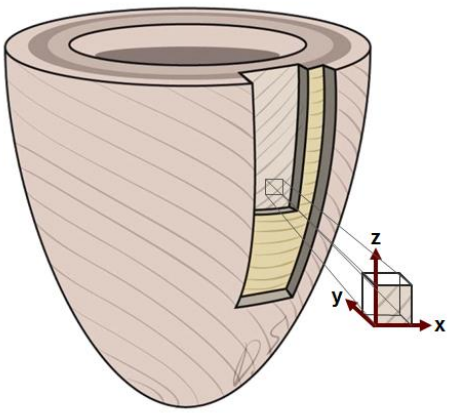

Figure 1. Schematic showing myocardial fiber orientation in a given voxel of left ventricle

However, this underlying fiber architecture has been implied using methods that rely on destructive histological sectioning for conventional microscopy to directly visualize heart muscle fibers.[1,3] Diffusion magnetic resonance (MR) tractography measures the aggregate motility of water molecules as they diffuse within a tissue and fundamentally assumes that the restriction of this motility reflects underlying microstructures. Diffusion MR tractography has been the workhorse in understanding the white matter structure of the brain and elucidate novel structural connectivity in humans.[4-7] Recent technological advances have made it possible for diffusion MRI to be applied in a beating human heart allowing for clinical applications.[8-10] Currently, the ability of diffusion MR tractography to delineate tissue microstructure of heart has not been fundamentally validated because there lacks verification from a direct comparison with 3-dimensional (3D) non-destructive histology of an intact heart. Histologic validation of diffusion MR tractography will enable researchers to investigate the microstructural change of myocardium according to various diseased by providing solid evidence for integrity of diffusion MR tractography, and this will eventually improve understanding of the fundamental heart structure-function relationships in both normal development and cardiovascular disease progression.

Tissue-clearing techniques are promising novel technologies capable of delivering intact molecular phenotyping imaging that may potentially address the current limitations of studying heart microstructure.[11,12] These techniques clear the intact tissue of light-scattering lipids. However, all previously reported tissue-clearing techniques have been optimized for the brain, which differs from the heart and therefore requires adjustment for cardiac application.[13] Additionally, the heart is typically larger than the brain in small animals, increasing the technical challenge of achieving full optical transparency.[14] One advantage of applying tissue-clearing techniques in the heart compared with the brain is the relative homogeneity of the tissue type in which the heart is mostly composed of myocytes.[15] Because both connective tissue and cardiomyocytes, which consists of most of the myocardium component, are aligned with same direction making a laminar structure,[2] simple auto-fluorescence of non-specific proteins in the myocardium could directly reveal the myocardial fiber structures of the heart once the tissue is sufficiently cleared. However, tissue-clearing techniques cannot be performed in vivo limiting its potential for clinical application beyond pathology. Instead, tissue-clearing techniques can be used to validate an indirect, non-destructive imaging technology capable of reflecting heart structure in a clinical setting such as diffusion MR tractography.

Therefore, the current aims of the study are first, to accomplish the first application of the tissue-clearing technique in intact normal mouse hearts using tissue-clearing technique-based lipid clearing of hearts combined with a

light-sheet based microscopic optical imaging, and second, to confirm the histological integrity of cardiac diffusion MR tractography in quantitative assessment of myocardial microstructure in both normal and diseased model by using the tissue-clearing technique.

II. MATERIALS AND METHODS

1. Mice animal model

8 weeks old male C57/B6 mice were used.

A. Control group

For the control group, male C57/B6 mice (n=7) were sacrificed at 12 weeks old to match the ischemic model.

B. Ischemic heart failure model

Eight-week-old male C57/B6 mice (n=8) were anesthetized with 2% isoflurane inhalation using an isoflurane delivery system. After making a small skin cut (1.2 cm) over the chest, the major and minor pectoral muscle were dissected and retracted. The fourth intercostal space was exposed. With a mosquito clamp, a small hole was made at the fourth intercostal space to open the pericardium. The left coronary artery was located and ligated approximately 1mm from its origin using a 6-0 silk suture. If the anterior wall of the left ventricle turns pale, the ligation was thought to be successful. The heart was placed back into the intrathoracic space and muscle and the skin was closed. Ischemic model mice were sacked 30 days after the surgery to allow myocardial

remodeling. The formation of ischemic heart failure and cardiac remodeling was confirmed by echocardiography immediately before sacrifice.

C. Non-ischemic heart failure model

Non-ischemic heart failure model (n=7) was constructed using doxorubicin (DOX) induced chronic cardiac dysfunction. Doxorubicin 9mg/kg was intraperitoneally given to C57/B6 mice weighing 25 to 35g every 10 days for 3 times (cumulative dose 27mg/kg).[16] Mice were sacked after 30 days from the initial DOX administration to allow time for cardiac remodeling. The formation of heart failure and cardiac remodeling was confirmed by echocardiography before sacrificing the animal.

3. Harvesting of the heart and process of tissue-clearing technique

C57BL/6 mice were anaesthetized with zoletil (Virbac, Carros, France) and rompun (Bayer, Kansas city, Missouri, USA) and perfused with hydrogel monomer solutions, a mixture of 4% (wt.) paraformaldehyde (1.04005.1000, Millipore, Darmstadt, Germany), 4% (wt./vol) acrylamide (A8887, Sigma-Aldrich, St.Louis, Missouri, USA), 0.25% (wt./vol) VA-044 (017-19362, Wako, Tokyo, Japan) and phosphate-buffered saline (PBS). Hearts were extracted and incubated in hydrogel monomer solution at 4℃ for 3 days. Polymerization reaction was carried out by increasing the temperature to 37℃ for 3 hours using an Easy-Gel system (EG-1001, Live Cell Instrument, Seoul, Korea).

For clearing, clearing buffer, a mixture of sodium borate buffer (200mM, pH8.5) containing 4% (wt./vol) SDS (L3771, Sigma-Aldrich, St.Louis, Missouri, USA), was circulated. The heart was scanned ~~for~~ with diffusion MR tractography. After MR scanning, 100V was applied across the heart samples at 37℃ for 3 days using the Life Canvas (EC-1001, Live Cell Instrument, Seoul, Korea). After clearing, heart samples were washed in PBS at 37℃ for 2 days. Finally, heart samples were incubated in EZ-index (EI-Z1001, Live Cell Instrument, Seoul, Korea) for matching refractory index.

4. Diffusion MR tractography acquisition

After initial perfusion and polymerization, each heart was placed in a 15ml tube filled with the clearing buffer solution. A collection of twelve diffusion-weighted (b=1000s/mm^2) and one non-diffusion-weighted (b=0s/mm^2) single spin echo MRI[16] images was acquired on a 9.4T small animal scanner (BioSpec 94/20 USR, Bruker BioSpin, Rheinstetten, Germany) with the same imaging parameters (repetition time (TR)=8750ms, echo time (TE)=36ms, number of excitations (NEX)=5, spatial resolution=125㎛ x 125㎛ x 300㎛, scan time=14hours).

5. Diffusion MR tractography image analysis

Diffusion MR tractography tensor analysis[17,18] was performed on the acquired diffusion dataset at each voxel using software developed on Matlab (Mathworks, Natick, Massachusetts, USA). Briefly, a log-linear least squares fit was used to yield the apparent diffusion coefficients (D_{xx}, D_{yy}, D_{zz}, D_{xy}, D_{xz}, D_{yz})

of the self-diffusion tensor defined below:

$$\begin{bmatrix} D_{xx} & D_{xy} & D_{xz} \\ D_{xy} & D_{yy} & D_{yz} \\ D_{xz} & D_{yz} & D_{zz} \end{bmatrix}$$

Eigenvalue decomposition was performed to yield the eigenvectors and eigenvalues. The eigenvector associated with the larges eigenvalue (primary eigenvector) of the estimated self-diffusion tensor at each voxel was assumed to be parallel to the myocardial fiber orientation.[19-21] Helix angle (HA) was calculated using the same geometric definition as Streeter, et al,[1] with local tangent vector being defined from the center of mass of the left ventricular blood pool to the voxel of interest for each short axis plane. For 3D visualization, diffusion MR tractography was performed using a FACT algorithm.[22]

6. Optical imaging of cleared mouse heart

Optical images of clarified intact mouse hearts were mounted with the apex facing the objective lens. The hearts were imaged using a light-sheet fluorescence microscope (Lightsheet Z.1,Carl Zeiss Microscopy Co, Ltd. , Oberkochen, Germany; stack size, 4.823mm; 2.283㎛ x 2.283㎛ in-plane resolution; step size 7.67㎛) equipped with the x5 objective (EC Plan-Neofluar 5x, Carl Zeiss Microscopy Co, Ltd., Oberkochen, Germany) at 638-nm excitation.

7. Optical image analysis

Raw 3D optical images were filtered to remove any residual stripe-like

shadow artifacts.[23] Conventional 3D structure tensor analysis was performed on the filtered images to calculate myocardial fiber orientation at each voxel.[24-26] Briefly, image gradients (f_x, f_y, f_z) of the optical images were calculated in three dimensions using a Sobel filter and populating the following structure tensor:

$$\begin{bmatrix} f_x f_x & f_x f_y & f_x f_z \\ f_y f_x & f_y f_y & f_y f_z \\ f_z f_x & f_z f_y & f_z f_z \end{bmatrix}$$

Eigenvalue decomposition can be performed on the structure tensor to yield a primary eigenvector, which reflects the myocardial fiber orientation.

8. Comparison of myocardial fiber architecture between cleared 3D optical imaging and diffusion MRI

HA maps were used to compare cleared 3D optical imaging and diffusion MR tractography. For each heart sample, the 3D optical images were down-sampled to match the resolution of the diffusion MR tractography. Binary masks were created for both optical and MR tractography-based HA maps using simple thresholding to identify the myocardium from background. Co-registration was performed on the binary masks using conventional non-rigid, intensity-based mutual information algorithm[27] to obtain the transform matrix that maps the optical binary mask to the MR tractography binary mask. The transform matrix was applied to the HA maps and voxel-wise comparison was performed only including voxels with myocardium (i.e. excluding collagenous scar tissue). The global HA transmurality (HAT) was calculated for each heart defined as the mean of the fitted slopes of HA against

transmural depth along 20 equidistant radial projections (areas of scar tissue excluded) in the short axis plane for all slices. The global HAT is a reflection of the degree of helical microstructure present with lower absolute HAT indicating less helical winding.

9. Statistical analysis

Continuous variables are presented as mean ± standard error. Non-parametric Wilcoxon test was performed to compare means. Analysis of Bland-Altman was performed to quantify the agreement between diffusion MRI and optical, and linear regression analysis was used to examine the relationship between helix angle calculated from diffusion MRI and optical imaging. All comparisons were two sided and $p<0.05$ was considered statistically significant, with 95% confidence interval. Statistical analyses were performed using SPSS version 23 (SPSS, Inc., Chicago, IL) and MedCalc version 16.4.3 software (MedCalc Software, Ostend, Belgium).

III. RESULTS

1. Intact adult mouse heart 3D optical imaging

The tissue-clearing technique was applied in 7 normal, 8 ischemic and 7 non-ischemic adult mouse hearts. **Figure 2** reveals the effectiveness of applying the tissue-clearing technique to murine heart tissue in removing light scattering lipids.

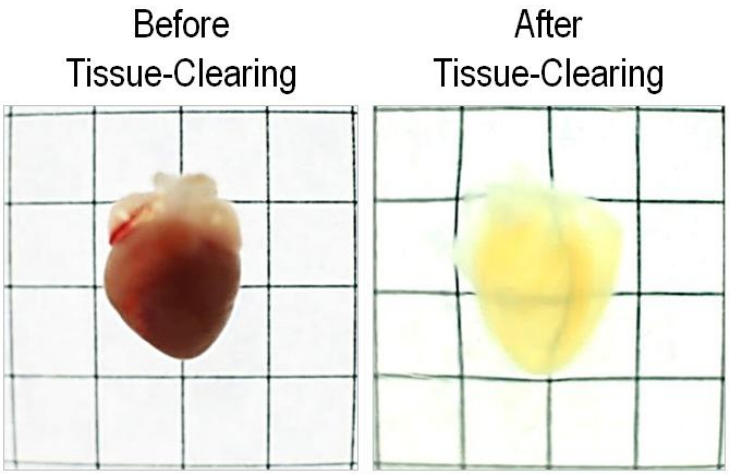

Figure 2. Mouse heart before (left) and after (right) tissue-clearing

Myocardial fiber laminar structures of about 15-20㎛ in size can directly be visualized with the endogenous auto-fluorescence of the myocardial tissue . Further image processing of the raw optical images using Sobel filters to accentuate edges and image intensity gradients increased the contrast of the myocardial fiber structure. These image intensity gradient processed images served as inputs to 3D structure tensor analysis to quantitatively calculate fiber orientation. Fiber orientation represented in red, green, and blue (RGB) color map (**Figure 3**) show fibers twisting around the blood pool in the short axis plane with epicardium and endocardium having a significant through-plane component consistent with the helical structure.

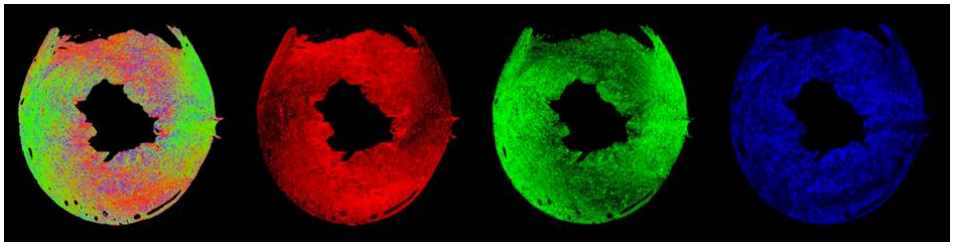

Figure 3. Quantitative fiber orientation mapping after structure tensor analysis map represents primary fiber orientation in red, green, and blue (RGB) color map. RGB is mapped to left-right, up-down, and in-out orientations, respectively.

This is also confirmed by a transmural virtual sectioning of the same optical image (**Figure 4**) that reveals the presence of right handed helical oriented layers smoothly transitioning to left handed helical orientation from endocardium to epicardium, respectively.

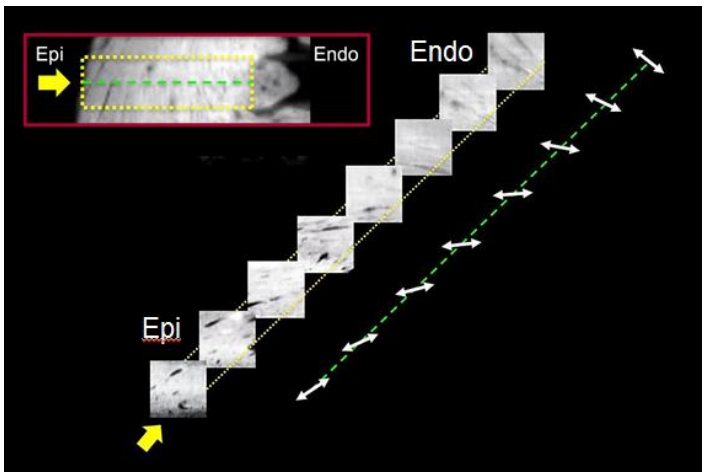

Figure 4. Helical rotation of fiber axis from epicardium to endocardium revealed by virtual transmural sectioning.

Helix angles were quantified and plotted against transmural depth to further demonstrate the transmural transition of right handed to left handed helical orientation.

2. Intact adult mouse heart diffusion MRI imaging

After extraction and before clearing, all hearts were scanned with MR to obtain diffusion MR tractography images. At each voxel, the diffusion MRI images were reconstructed to model the self-diffusion tensor and myocardial fiber orientation was assumed to be parallel to the primary eigenvector of the tensor. Similar to optical imaging of the cleared myocardium, diffusion MR tractography qualitatively also revealed twisting of fibers around the blood pool in the short axis plane with significant through-plane directionality in the endocardium and epicardium layers (**Figure 5**).

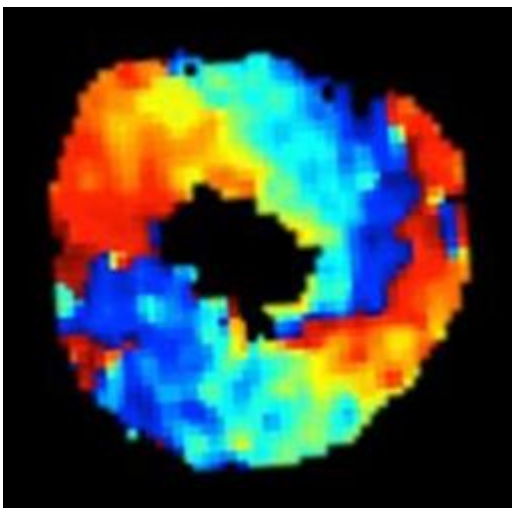

Figure 5. Short axis plane of diffusion MR tractography

To compensate for the coarse (1/2600 worse) resolution of diffusion MRI (125x125x300μm^3) compared with the 3D optical imaging (2.28x2.28x7.67 μm^3), 3D tractography of the diffusion tensor data which subdivided each voxel into 1000 sub-voxels was used to further qualitatively visualize the helical twisting of the fibers from apex to base.

3. Comparison of 3D optical-based and diffusion MR tractography-based helix angle

Down-sampling and co-registration were applied to the myocardial fiber orientation maps generated by 3D optical imaging to myocardial fiber orientation maps generated by diffusion MR tractography. The HA was calculated using the myocardial fiber orientation at each voxel for all subjects and both imaging modalities.

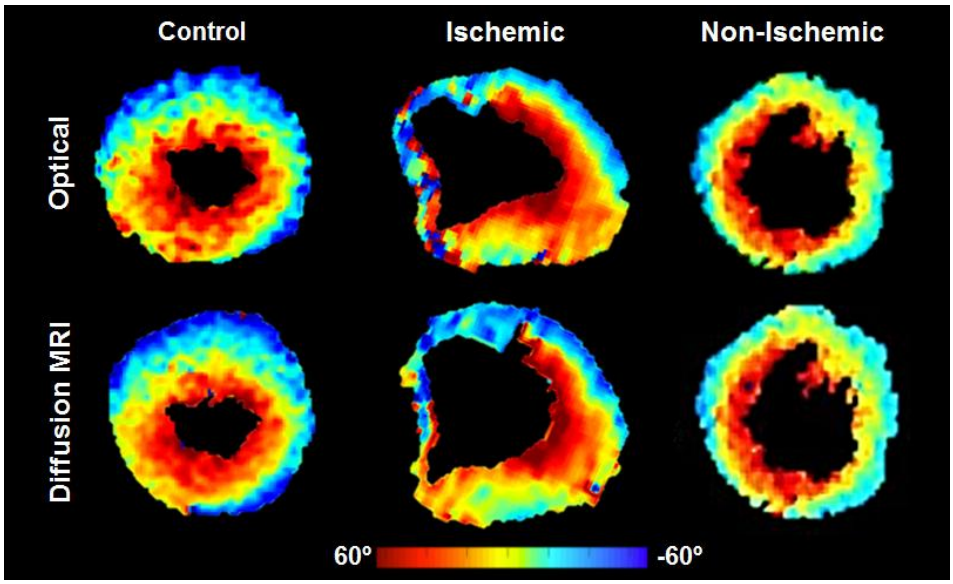

Figure 6. Representative short axis HA maps of control, ischemic and

non-ischemic heart failure model mice hearts

For both imaging modalities, smooth transmural transition of the HA from epicardium to endocardium was observed in controls and perturbed transition in ischemic hearts near the infarct area and non-ischemic hearts (Figure 6).

Control hearts (Diffusion MR: 1.3±0.2°/% transmural depth and optical: 1.4±0.3°/% transmural depth) exhibited more helical microstructure with a significantly higher magnitude of global HAT than either ischemic (Diffusion MRI: 0.8±0.1°/% transmural depth and optical: 0.8±0.2°/% transmural depth) or non-ischemic (Diffusion MRI: 0.8±0.1°/% transmural depth and optical: 0.9±0.2°/% transmural depth) hearts (all $p<0.001$). Note for ischemic hearts, scarred infarcted lesions were excluded from the comparison analysis due to low auto-fluorescence signal, which resulted in unreliable structure tensor analysis compared to the remote myocardium.

Comparing between optical-based and diffusion-MR tractography based global HAT, significant agreement ($R^2 = 0.803$, $p<0.001$) can be observed across all heart samples. Within each group significant agreement ($R^2 = 0.809$, $R^2 = 0.702$, and $R^2 = 0.540$ for control, ischemic, and non-ischemic groups, respectively, all $p<0.05$) was also found between optical-based and diffusion-MR tractography based HAT.

The Bland-Altman limits of agreement (95% CI) for the HAT by

diffusion MRI and 3D histology were 0.60 to 1.38 for all samples (-0.29 to 0.21 for controls, -0.38 to 0.28 for ischemics, and -0.31 to 0.44 for non-ischemics), which can be considered acceptable for the validation of diffusion MR tractography (Figure 7).

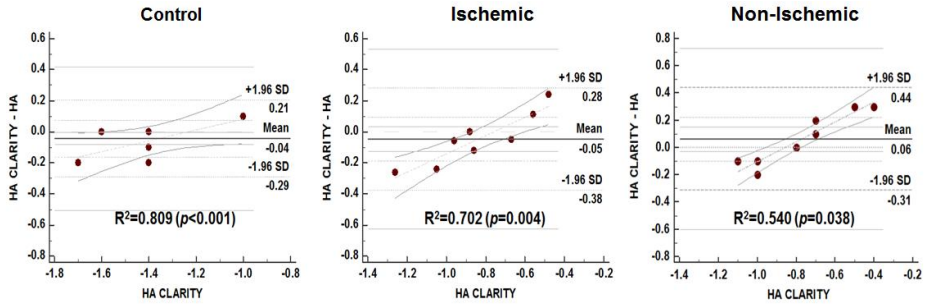

Figure 7. Bland-Altman and correlation plots demonstrating the similarity between the optical-based and diffusion MR tractography-based myocardial fiber helix angle transmurality estimation

IV. DISCUSSION

The result of current study supports the existence of a multi-layered helical structure in the left ventricle of the mammalian heart, which was directly visualized by the 3D histology with the use of the tissue-clearing technique. The intact 3D microstructure of the myocardium by diffusion MR tractography was also successfully constructed. The complex 3D microstructure of the heart have never been directly visualized before, largely due to the complex architecture of myocardial tissue, technical limitations of previous imaging modality, and more

importantly, the destructive techniques which traditionally have been used to examine it. Identification of true 3D myocardial fiber orientation using conventional approaches such as 2D histology is fundamentally flawed because the 3D data had to be reconstructed from images of thin slices, in which the preparation using destructive sectioning can disrupt the myocardial microstructure. In addition, quantification of 3D fiber-orientation with 2D histology is laborious and limited with fiber angles only being identified in tangential sections.[28] As a result, it has been extraordinarily challenging to perform histologic assessment without dissecting and thus compromising intact fiber orientation of the heart. However with the use of a tissue clearing technique, the myocardial fiber architecture was visualized in its intact form, without destructive tissue sectioning.

As shown in the comparison of three different study models, the myocardial fiber architecture is perturbed in the presence of ischemic and non-ischemic disease. Because myocardial tissue structure is intimately linked to heart function, both changes considerably as disease progresses. However, to date, there was no optimal imaging modality to prove the complete and consistent description of myocardial structure, and its deformation during the progression of disease. Consequently, the disruption in myocardial structure has been indirectly assessed through detection of scar tissue manifested in myocardial thinning or late gadolinium enhancement in MRI.[29,30] The present study illustrated both 3D histology and diffusion MR tractography were able to

directly characterize the myocardial fiber architecture of a diseased myocardium as opposed to indirectly focusing on the scar region. Both imaging modalities were in agreement in demonstrating the loss of transmural helical myocardial fiber architecture in the presence of disease.

Most importantly, the accuracy of diffusion MR tractography in assessing the myocardial microstructure was validated. The histologic validation of diffusion MR tractography has been limited because since diffusion MR tractography-based fiber orientations reflect the 3D microstructure and conventional histology requires destructive sectioning to acquire 2D optical images.[31] All prior research has been based on inherently tissue-destructive conventional techniques, such as serial histological sections, which limit analysis to small volumes of heart.[32] Furthermore, the process of destructive sectioning may modify or damage the myocardial fiber microstructure fundamentally casting doubt on whether conventional 2D histology is appropriate ground truth reference for diffusion MR tractography.[33,34] By comparing the diffusion MRI with tissue-clearing technique prepared 3D histology, the ability of diffusion MR tractography in yielding myocardial fiber orientations reflective of the myocardial architecture in an intact myocardium was demonstrated. Although a certain degree of tissue swelling is unavoidable during the process of polymerization, the myocardial fiber orientation is maintained enabling direct comparison of fiber orientations between 3D histology and diffusion MR tractography across the entire

myocardium. More importantly, established image analysis tools such as non-rigid co-registration can be reliably and efficiently used to compare the acquired 3D volumes acquired by 3D histology and diffusion MR tractography across millions of pixels.

Although there has been effort to non-invasively describe the tissue characterization over disease progression,[35-37] the clinical use of computed tomography, echocardiography, and even conventional cardiac MR tractography have been confined due to the limitations including requirement of contrast, low spatial resolution, long acquisition time, or risk of radiation exposure. Cardiac diffusion MR tractography has already become an established method for the characterization of myocardial microstructure in animal models.[38] In this context, diffusion MR tractography may be an alternative or supplemental method to T1 mapping for the detection and quantification of diffuse fibrosis.

V. CONCLUSION

In this study, the tissue-clearing technique, novel 3D histology technique, was successfully accomplished using mice cardiac tissue, which revealed helical myocardial structure of the myocardium. Furthermore, this same helical myocardial architecture can also be ascertained with diffusion MRI, a non-invasive medical imaging modality capable of in vivo imaging. By establishing concordance between 3D histology and diffusion MRI in yielding myocardial fiber architecture, diffusion MRI-based myocardial fiber orientation

characterization provides a promising tool for in vivo interrogation of the microstructural response of the myocardium in various cardiac diseases.

REFERENCES

1. Streeter DD, Spotnitz HM, Patel DP, Ross J, Sonnenblick EH. Fiber orientation in the canine left ventricle during diastole and systole. Circulation research 1969;24:339-47.
2. Stephenson RS, Agger P, Lunkenheimer PP, Zhao J, Smerup M, Niederer P, et al. The functional architecture of skeletal compared to cardiac musculature: Myocyte orientation, lamellar unit morphology, and the helical ventricular myocardial band. Clinical Anatomy 2015.
3. Streeter Jr DD, Vaishnav RN, Patel DJ, Spotnitz HM, Ross Jr J, Sonnenblick EH. Stress distribution in the canine left ventricle during diastole and systole. Biophysical Journal 1970;10:345.
4. Tuch DS, Reese TG, Wiegell MR, Wedeen VJ. Diffusion MRI of complex neural architecture. Neuron 2003;40:885-95.
5. Sporns O. From simple graphs to the connectome: networks in neuroimaging. Neuroimage 2012;62:881-6.
6. Le Bihan D. Looking into the functional architecture of the brain with diffusion MRI. Nature Reviews Neuroscience 2003;4:469-80.
7. McNab JA, Edlow BL, Witzel T, Huang SY, Bhat H, Heberlein K, et al. The Human Connectome Project and beyond: initial applications of

300mT/m gradients. Neuroimage 2013;80:234-45.

8. Reese TG, Weisskoff RM, Smith RN, Rosen BR, Dinsmore RE, Wedeen VJ. Imaging myocardial fiber architecture in vivo with magnetic resonance. Magnetic Resonance in Medicine 1995;34:786-91.

9. Gamper U, Boesiger P, Kozerke S. Diffusion imaging of the in vivo heart using spin echoes–considerations on bulk motion sensitivity. Magnetic Resonance in Medicine 2007;57:331-7.

10. Nguyen C, Fan Z, Sharif B, He Y, Dharmakumar R, Berman DS, et al. In vivo three-dimensional high resolution cardiac diffusion-weighted MRI: A motion compensated diffusion-prepared balanced steady-state free precession approach. Magnetic resonance in medicine 2014;72:1257-67.

11. Chung K, Wallace J, Kim S-Y, Kalyanasundaram S, Andalman AS, Davidson TJ, et al. Structural and molecular interrogation of intact biological systems. Nature 2013;497:332-7.

12. Richardson DS, Lichtman JW. Clarifying tissue clearing. Cell 2015;162:246-57.

13. Kolesová H, Čapek M, Radochová B, Janáček J, Sedmera D. Comparison of different tissue clearing methods and 3D imaging techniques for visualization of GFP-expressing mouse embryos and embryonic hearts. Histochemistry and cell biology 2016:1-12.

14. Hayamizu TF, Baldock RA, Ringwald M. Mouse anatomy ontologies:

enhancements and tools for exploring and integrating biomedical data. Mammalian Genome 2015;26:422-30.

15. Banerjee I, Fuseler JW, Price RL, Borg TK, Baudino TA. Determination of cell types and numbers during cardiac development in the neonatal and adult rat and mouse. American Journal of Physiology-Heart and Circulatory Physiology 2007;293:H1883-H91.

16. Pacher P, Liaudet L, Bai P, Mabley JG, Kaminski PM, Virág L, et al. Potent metalloporphyrin peroxynitrite decomposition catalyst protects against the development of doxorubicin-induced cardiac dysfunction. Circulation 2003;107:896-904.

17. Basser PJ, Mattiello J, LeBihan D. Estimation of the effective self-diffusion tensor from the NMR spin echo. Journal of Magnetic Resonance, Series B 1994;103:247-54.

18. Basser PJ, Pajevic S, Pierpaoli C, Duda J, Aldroubi A. In vivo fiber tractography using DT-MRI data. Magnetic resonance in medicine 2000;44:625-32.

19. Mekkaoui C, Reese TG, Jackowski MP, Bhat H, Sosnovik DE. Diffusion MRI in the heart. NMR in Biomedicine 2015.

20. Sosnovik DE, Wang R, Dai G, Reese TG, Wedeen VJ. Diffusion MR tractography of the heart. Journal of Cardiovascular Magnetic Resonance 2009;11:1.

21. Goergen CJ, Sosnovik DE. From molecules to myofibers: multiscale

imaging of the myocardium. Journal of cardiovascular translational research 2011;4:493-503.

22. Mori S, Crain BJ, Chacko V, Van Zijl P. Three-dimensional tracking of axonal projections in the brain by magnetic resonance imaging. Annals of neurology 1999;45:265-9.

23. MŘnch B, Trtik P, Marone F, Stampanoni M. Stripe and ring artifact removal with combined wavelet—Fourier filtering. Optics express 2009;17:8567-91.

24. Budde MD, Frank JA. Examining brain microstructure using structure tensor analysis of histological sections. Neuroimage 2012;63:1-10.

25. Khan AR, Cornea A, Leigland LA, Kohama SG, Jespersen SN, Kroenke CD. 3D structure tensor analysis of light microscopy data for validating diffusion MRI. NeuroImage 2015;111:192-203.

26. Bigun J. Optimal orientation detection of linear symmetry. 1987.

27. Choe AS, Gao Y, Li X, Compton KB, Stepniewska I, Anderson AW. Accuracy of image registration between MRI and light microscopy in the ex vivo brain. Magnetic resonance imaging 2011;29:683-92.

28. Harrington KB, Rodriguez F, Cheng A, Langer F, Ashikaga H, Daughters GT, et al. Direct measurement of transmural laminar architecture in the anterolateral wall of the ovine left ventricle: new implications for wall thickening mechanics. American Journal of Physiology-Heart and Circulatory Physiology 2005;288:H1324-H30.

29. Green JJ, Berger JS, Kramer CM, Salerno M. Prognostic value of late gadolinium enhancement in clinical outcomes for hypertrophic cardiomyopathy. JACC: Cardiovascular Imaging 2012;5:370-7.

30. Shah DJ, Kim HW, James O, Parker M, Wu E, Bonow RO, et al. Prevalence of regional myocardial thinning and relationship with myocardial scarring in patients with coronary artery disease. JAMA 2013;309:909-18.

31. Gilbert SH, Benoist D, Benson AP, White E, Tanner SF, Holden AV, et al. Visualization and quantification of whole rat heart laminar structure using high-spatial resolution contrast-enhanced MRI. American Journal of Physiology-Heart and Circulatory Physiology 2012;302:H287-H98.

32. Hales PW, Schneider JE, Burton RA, Wright BJ, Bollensdorff C, Kohl P. Histo-anatomical structure of the living isolated rat heart in two contraction states assessed by diffusion tensor MRI. Progress in biophysics and molecular biology 2012;110:319-30.

33. Kim S, Chi-Fishman G, Barnett AS, Pierpaoli C. Dependence on diffusion time of apparent diffusion tensor of ex vivo calf tongue and heart. Magnetic resonance in medicine 2005;54:1387-96.

34. Scott AD, Nielles-Vallespin S, Ferreira PF, McGill LA, Pennell DJ, Firmin DN. The effects of noise in cardiac diffusion tensor imaging and the benefits of averaging complex data. NMR in Biomedicine 2016;29:588-99.

35. Danad I, Szymonifka J, Schulman-Marcus J, Min JK. Static and dynamic assessment of myocardial perfusion by computed tomography. Eur Heart J Cardiovasc Imaging 2016:jew044.

36. Omar AMS, Bansal M, Sengupta PP. Advances in Echocardiographic Imaging in Heart Failure With Reduced and Preserved Ejection Fraction. Circulation Research 2016;119:357-74.

37. Puntmann VO, Peker E, Chandrashekhar Y, Nagel E. T1 Mapping in Characterizing Myocardial Disease A Comprehensive Review. Circulation Research 2016;119:277-99.

38. Sosnovik DE, Mekkaoui C, Huang S, Chen HH, Dai G, Stoeck CT, et al. Microstructural impact of ischemia and bone marrow–derived cell therapy revealed with diffusion tensor magnetic resonance imaging tractography of the heart in vivo. Circulation 2014;129:1731-41.

APPENDICES

ABSTRACT (IN KOREAN)

심장의 자기공명영상 소견과 투명화된 생체 밖 마우스 심장의 비교를 통한 자기공명영상의 심근 주행 방향 감별의 정확도 평가

<지도교수 장혁재 >

연세대학교 대학원 의학과

이상은

심근은 일정한 방향성을 가지고 배열되어 있으며, 이는 질병의 진행에 따라 변화할 것으로 예측되나, 이를 비침습적으로 평가할 수 있는 방법은 없었다. 본 연구는, 새로 개발된 자기공명영상 기법이 심근의 주행방향을 정확히 측정할 수 있는 지에 대하여 심근의 투명화 기법을 사용하여 자기공명영상의 정확도를 평가하고자 한다. 7마리의 대조군, 8마리의 허혈성 심부전 모델, 7마리의 비허혈성 심부전 모델 마이스를 대상으로 실험을 진행하였으며, 자기공명영상으로 획득한 심근의 주행방향이 병리학적으로 처리된 투명화된 심장에서 얻은 심근의 주행방향과 일치함을 밝혔다. 본 연구를 통하여 심장 자기공명영상이 심근 주행 방향을 정확히 감별할 수 있음이 밝혀졌으며, 추후 임상에 응용될 수 있는 증거로서 제시될 수 있을 것으로 기대한다.

핵심되는 말 : 심장 자기공명 영상, 심근 주행 방향